Morphological and molecular comparison of three centric diatoms (Bacillariophyceae: Chaetoceros) isolated from the coast of Eastern Thailand

Rachanimuk Hiransuchalert (rachanimuk@buu.ac.th)
Burapha University
Maliwan Kutako
Burapha University
Sarayut Watchasit
Burapha University
Mookthida Kaewduang
Burapha University
Pakawan Setthamongkol
Burapha University
Parinya Chindudsadeegul
Burapha University
Vichaya Gunbua
Burapha University
Somtawin Jaritkhuan
Burapha University

Research Article

Keywords: Chaetoceros, nuclear 18S rDNA, sequencing, RAPD, NMR

Posted Date: March 16th, 2022

DOI: https://doi.org/10.21203/rs.3.rs-1406725/v1

Abstract

The objective of this study was to identify *Chaetoceros* species using microscopic observations, sequence analysis of 18S rDNA, random amplified polymorphic DNA (RAPD) barcoding and nuclear magnetic resonance (NMR) spectroscopy. *Chaetoceros* were obtained from three different algae laboratories: Center of Excellence for Marine Biotechnology (CEMB), Chanthaburi Coastal Fisheries Research and Development (CHAN) and Institute of Marine Science, Burapha University (BIM). Genomic DNA for the RAPD analysis was extracted using the phenol-chloroform method, followed by 18S rDNA amplification. The 18S rDNA sequence analysis showed that *Chaetoceros* CEMB was most similar to *C. gracilis* (e-value = 0.0, identity = 98%), *Chaetoceros* CHAN was most similar to *C. debilis* (e-value = 0.0, identity = 99%) and *Chaetoceros* BIM was most similar to *C. debilis* (e-value = 0.0, identity = 98%). The RAPD results revealed differences in the three *Chaetoceros* isolates with polymorphisms between 30.43% and 60.00%, and *Chaetoceros* CEMB showed high polymorphic bands. Scanning electron microscopy revealed that *Chaetoceros* CEMB were larger and had larger setae compared with the other isolates ($P < 0.05$). The results of the NMR characterization of metabolites were consistent with the results of the sequence and morphological analyses. The concentrations of several metabolites, including chlorophyll c_1, chlorophyll a, myo-inositol, fucoxanthin, astaxanthin, lutein and zeaxanthin, were lower in *Chaetoceros* CEMB than in *Chaetoceros* BIM and CHAN. However, high concentrations of fatty acids, such as oleic acid, linoleic acid, α-linolenic acid and arachidic acid, were observed in all isolates. Generally, the results of this study will aid future studies examining the diversity of *Chaetoceros* in various culture environments.

Introduction

Ocean's diatoms are an important group of eukaryotic phytoplankton that dominate phytoplankton communities in upwelling regions and at high latitudes (Benoiston et al. 2017). Diatoms are commonly fed to the larvae of aquatic animals in the aquaculture industry. The main species of diatoms used as food in the shrimp aquaculture industry are *Chaetoceros*, *Thalassionema*, *Closterium* and *Thalassiosira*. *Chaetoceros* is one of the most abundant and widespread diatom genera with approximately 400 species described (Rines and Theriot 2003). It is an ecologically important genus of marine planktonic diatoms that are found in coastal and upwelling regions (Jensen and Moestrup 1998). *Chaetoceros* has been used for biofuel production because of its high growth rates and high lipid yield (Spaulding and Edlund 2008). Their utility stems in part from their small size and their high n-3 polyunsaturated fatty acids (HUFA) content; these properties also make *Chaetoceros* an important source of lipids and fatty acids for marine fish, bivalves and crustaceans (Xu et al. 1993; Zhou et al. 2007). Among *Chaetoceros* species, *C. muelleri* and *C. gracilis* have been cultivated for use as food for *Litopenaeus vannamei* larvae (Sangha et al. 2000). Rotifers fed *C. gracilis* showed increased viability, larger size and low ciliate contamination (Knu 2004). Freeze-dried *C. muelleri* is commercially available as feed for shrimp, sea cucumbers and oysters and can be used in green water techniques in fish larviculture (e.g., https://algae.proviron.com). Previous research has indicated that *C. muelleri* shows antimicrobial activity against *Staphyloccocus aureus*, *Escherichia coli* and *Candida albicans* (Mendiola et. al. 2007). *C. gracilis* has the ability to produce high-quality fatty acids for the lipid industry (Rika Partiwi et. al. 2009).

Diatom cells have a silica cell wall in the form of two shells called the frustule. Microscopic identification of diatoms is based on frustule shape. Although there are several detailed taxonomic descriptions of the microstructure of their silica frustules, diatoms are time-consuming and difficult to identify. Molecular tools permit diatom biodiversity to be more easily estimated at all taxonomic levels.

DNA barcoding is a fast, accurate and standardized method for species-level identification that uses short DNA sequences. DNA barcoding has become an effective tool for assessing global biodiversity patterns and permits non-taxonomic biologists to diagnose species challenging to identify (Siddall et al. 2009). Diatoms are an ideal model group for developing DNA barcoding methods that provide easy-to-use, standardized and fast identification tools. Nuclear 18S rRNA is the most widely used sequence that has been used in phylogenetic analyses of diatoms (Evans et al. 2007). Random amplified polymorphic (RAPD) markers are also highly useful for the study of populations within species because of their low cost and the fact that they do not require large sample sizes to generate preliminary results (Godhe et al. 2006).

In this study, the morphological and molecular taxonomic characteristics of *Chaetoceros* isolated from the coast of Eastern Thailand were investigated through microscopic observations, DNA barcoding using RAPD-PCR techniques, and molecular phylogenetic approaches using 18S rDNA. In addition, we present NMR patterns as well as chemical information on *Chaetoceros*.

Materials And Methods

Diatom propagation and culturing system

Chaetoceros were obtained from three different algae laboratories: the Center of Excellence for Marine Biotechnology (CEMB), Faculty of Science, Chulalongkorn University, which originally isolated *Chaetoceros* from natural sea water in Angsila, Chon Buri province (hereafter referred to as *Chaetoceros* CEMB); Institute of Marine Science, Burapha University (BIM), which originally isolated *Chaetoceros* from natural sea water in Bang Saen, Chon Buri (hereafter referred to as *Chaetoceros* BIM); and Chanthaburi Coastal Fisheries Research and Development (CHAN), Department of Fisheries, Ministry of Agriculture and cooperatives, which originally isolated *Chaetoceros* from natural sea water in Laemsing, Chanthaburi province (hereafter referred to as *Chaetoceros* CHAN).

Diatom culture procedures were carried out under sterile conditions to avoid contamination. The diatom samples from the laboratory collections were purified using the centrifugation and streaking method. The samples were washed 12 times by RO water (30 ppt salinity), followed by centrifugation at 2000× g for 1–2 min, and the supernatants were discarded every round. Each diatom strain was then aseptically streaked onto a sterile plate containing F/2 (Guillard 1975) media with water at 30 ppt salinity and 1.2–1.5% agar. The plate was incubated at 25°C until diatom colonies appeared. A single colony was transferred into test tubes containing 10 ml of fresh media. The diatom propagation process was first carried out in a 100-ml flask, followed by 500 ml in F/2 (Guillard 1975) media with water at 30 ppt salinity. The room was maintained at 25°C and under continuous illumination at a low light intensity (1000 lux). To accelerate growth, diatom cultures were vigorously aerated until they reached the stationary phase. Diatom cultures were then centrifugated at 12,000× g for 1–2 min, and the supernatants were discarded. The cells were kept at –20°C until DNA extraction.

Morphological observations

Monoclonal cultures of diatom strains were identified to the genus or species level by morphological features based on observations using a light and scanning electron microscope. For light microscopy, diatom cultures were treated with acid to prepare cleaned frustules. The slides were examined using light microscopy under a 100× oil immersion objective lens (model BX53, Olympus). For scanning electron microscopy, diatom cells were placed on glass plates coated with 0.5% Alcian blue, fixed with 2.5% glutaraldehyde in 0.1 M phosphate buffer saline (PBS) solution for 1 h and then washed with distilled water. Cells were further fixed under dark conditions with 1% osmium tetroxide in 0.1 M PBS solution for 1 h and then washed with distilled water. The samples were dehydrated in a graded ethanol series (70%, 80%, 90%, 95% and 100%) and dried using the critical point drying method. Finally, the samples were mounted onto stubs and sputter-coated with 99.99% pure gold. The specimens were examined under a scanning electron microscope (LEO1450VP, Zeiss, Oberkochen, Germany) with a 205-nm resolution at 10 kV. Morphological comparisons followed the procedures described in previous studies. Cell size (length, width and setae length, in μm) measurements of *Chaetoceros* were taken.

Genomic DNA extraction

High molecular weight genomic DNA (gDNA) was extracted from the washed diatom cells using the phenol-chloroform-proteinase K method (Sambrook and Russell 2001). Fifty nanograms of diatom cells were placed in a prechilled microcentrifuge tube containing 500 ml of the extraction buffer (100 mM Tris-HCl, 100 mM EDTA, and 250 mM NaCl; pH 8.0) and briefly homogenized with a micropestle. SDS (10%) and RNase A (10 mg/ml) solutions were added to a final concentration

of 1.0% (w/v) and 100 µg/ml, respectively. The mixture was then incubated at 37°C for 1 h. At the end of the incubation period, a proteinase K solution (10 mg/ml) was added to a final concentration of 100 µg/ml and further incubated at 55°C for 3–4 h. An equal volume of buffer-equilibrated phenol was added and gently mixed for 15 min. The solution was then centrifuged at 10,000 rpm for 10 min at room temperature. The upper aqueous phase was transferred to a newly sterile microcentrifuge tube. This extraction process was then repeated once with phenol:chloroform:isoamylalcohol (25:24:1) and twice with chloroform:isoamylalcohol (24:1). The aqueous phase was transferred into a sterile microcentrifuge. A one-tenth volume of 3 M sodium acetate (pH 5.2) was then added. DNA was precipitated by the addition of two volumes of prechilled absolute ethanol and mixed thoroughly. The mixture was incubated at –20°C for 2 h. The precipitated DNA was recovered by centrifugation at 12,000 rpm for 10 min at room temperature and washed twice with 1 ml of 70% ethanol (5 min and brief washes, respectively). After centrifugation, the supernatant was removed. The DNA pellet was air-dried and resuspended in 100 ml of TE buffer (10 mM Tris-HCl, pH 8.0 and 0.1 mM EDTA). The DNA solution was incubated at 37°C for 1–2 h and kept at 4°C until used.

RAPD-PCR analysis

Polymerase chain reaction (PCR) amplification was performed in 25-µl volumes containing 50 ng of genomic DNA; 2.5 µl of 10X *Taq* DNA polymerase buffer (FINNZYMES, Finland); 200 µM each of dATP, dGTP, dCTP, and dTTP; 0.2 µM primer (UBC101, 5'-GCGCCTGGAG-3' and OPB01, 5'-GTTTCGCTCC-3'); 2.0 mM $MgCl_2$; and 1.0 unit of *Taq* DNA polymerase. PCR thermocycling conditions were as follows: initial denaturation at 94°C for 3 min, followed by 40 cycles of denaturation at 94°C for 15 s; annealing at 36°C for 1 min and extension at 72°C for 1.30 min; and final extension at 72°C for 7 min. Twelve µl of PCR products were electrophoresed on a 2.0% (w/v) agarose gel using a 1-kb DNA ladder (Promega) for size comparison before being stored at –20°C.

PCR amplification, gene cloning and sequencing

The 18S rDNA locus from the genomic DNA of each diatom was amplified using universal diatom 18S rDNA-specific primers (Ki et al. 2009) (forward AT18F01, 5'-TACCTGGTTGATCCTGCCAGTAG-3' and reverse AT18R01, 5'-GCTTGATCCTTCTGCAGGTTCACC-3'). PCR amplification was carried out in 25-µl volumes containing 50 ng of genomic DNA; 2.5 µl of 10X *Taq* DNA polymerase buffer (FINNZYMES, Finland); 200 µM each of dATP, dGTP, dCTP, and dTTP; 0.2 µM of each primer; 2.0 mM $MgCl_2$; and 1.0 unit of *Taq* DNA polymerase. PCR thermocycling conditions were as follows: initial denaturation at 94°C for 3 min, followed by 35 cycles of denaturation at 94°C for 30 s; annealing at 50°C for 1 min and extension at 72°C for 1.30 min; and final extension at 72°C for 7 min. The PCR products were electrophoresed on 1.5% (w/v) agarose gel using a 1-kb DNA ladder (Promega) for size comparison before being stored at –20°C.

Successful amplification products were purified using NucleoSpin® Gel and PCR Clean-up (Germany), cloned into a pGEM®-T Easy vector (Promega) and transformed into *E. coli* strain JM109 cells. Plates were then left until the cell suspension was fully absorbed before being further incubated at 37°C overnight. Recombinant clones containing inserted DNA were white, whereas those without inserted DNA were blue. Insert sizes were verified using colony PCR (Sambrook and Russell 2001), and plasmid DNA was extracted from recombinant clones and unidirectionally sequenced (AITBiotech Pte. Ltd., Singapore). Complimentary nucleotides of both forward and reverse primers of 18S rDNA were identified. Nucleotide sequences were analyzed against molecular reference databases using the BLAST® algorithm (Basic Local Alignment Search Tool) (www.ncbi.nlm.nih.gov/BLAST); similarity was considered significant when the probability (E) value recovered was less than 10^{-4} (Altschul et al. 1990).

DNA sequence characteristics and phylogenetic analyses

Intraspecific variation in *Chaetoceros* was investigated by comparing the DNA similarities and genetic distances of 18S rDNA sequences. Multiple alignments were performed with each dataset using the ClustalW algorithm (Thompson et al. 1994). The

aligned sequences were trimmed at each end to the same length, and obvious base errors that were only found in single strands were manually removed. Identical positions of the aligned sequences were used. The corrected pairwise (*p*-) genetic distances were calculated using the Kimura 2-parameter model (MEGA 10.0, Tamura et al. 2007).

An 18S rDNA phylogeny was constructed using the unweighted pair group method with arithmetic mean and neighbor-joining algorithms (MEGA 10.0, Tamura et al. 2007) based on the Kimura two-parameter distance matrix; 1000 bootstrap replicates were performed to assess the reliability of the topology. The similarity of GenBank sequences and sequences obtained in our study were also compared. A total of 12 rDNA sequences from *Chaetoceros* were used in analyses. The 18S rDNA sequences were determined from eight *Chaetoceros* species: *C. calcitrans* (GenBank accession numbers AY485449, AY625894, EU240879, EU240880), *C. curvisetus* (AY229895), *C. debilis* (AY229896), *C. gracilis* (AY625895), *C. muellerii* (AY485453, AY625896), *C. neogracile* (EU090012), *C. rostratus* (X85391) and *C. socialis* (AY485446).

Sample preparation for NMR analysis

Approximately 10 mg of methanol crude extract was dissolved in 600 µL of deuterated acetone, which included the internal standard tetramethylsilane (TMS). The mixture was sonicated for 5 min and centrifuged at 3500 rpm for 5 min. Next, 550 µL of supernatant was collected with a pipette and placed in a 5-mm NMR tube. All experiments (1D and 2D experiments) were performed using a Bruker Avance III HD 400 MHz NMR spectrometer, equipped with a 5-mm BBFO probe (Double Resonance Broadband Observe with ^{19}F probe) at 25°C. The ^{1}H-NMR spectra of *Chaetoceros* extract were collected using the following parameters: pulse program zg30; relaxation delay 1 s; pulse width 8.90 µs; number of scans 64; sweep width 18 ppm; and center of spectrum 6.50 ppm. The ^{13}C-NMR spectrum of *Chaetoceros* extract was collected using the following parameters: pulse program zgpg30; relaxation delay 2 s; pulse width 7.50 µs; number of scans 8900; sweep width 240 ppm; and center of spectrum 100 ppm. Parameters of the 2D *J*-resolved NMR were as follows: pulse program jresgpprqf; relaxation delay 2 s; 128 increments; 16 transients; sweep width 18 ppm; and center of spectrum for ^{1}H was 8.0 ppm in both dimensions. The parameters for HMBC are as follows: pulse program hmbcetgpl3nd; relaxation delay 2 s; 512 increments; 84 transients; sweep width and center of spectrum for ^{1}H were 20.0 and 9.0 ppm, respectively. Sweep width and center of spectrum for ^{13}C were 240.0 and 100.0 ppm, respectively.

Results And Discussion

Growth pattern of Chaetoceros

Chaetoceros CHAN had the greatest cell numbers between day 3 (183×10^4 cell/mL) and day 6 (192×10^4 cell/mL) during the culture period (Fig. 1). The growth of *Chaetoceros* CHAN and *Chaetoceros* BIM exponentially increased during days 2–3, and *Chaetoceros* CEMB exponentially increased during days 3–5. At day 6, the numbers of cells of *Chaetoceros* CEMB and *Chaetoceros* BIM were 168×10^4 and 150×10^4 cell/mL, respectively.

Morphological characterization of Chaetoceros

Chaetoceros from this study were isolated from the Gulf of Thailand: *Chaetoceros* CEMB and *Chaetoceros* BIM were isolated from Chonburi province, and *Chaetoceros* CHAN was isolated from Chanthaburi province. The most abundant phytoplankton in the Central Gulf of Thailand are diatoms and blue-green algae (Kajonwattanakul et al. 2008).

Light microscope images are shown in Figs. 2a–c. The sizes of the three *Chaetoceros* isolates were small (ca. 5 µM). They were delicate and nearly square or rectangular in girdle view, with the pervalvar axis longer than the apical axis. Traditionally, the identification of diatoms at the species level has been based on morphological features determined with the aid of light microscopy, including the morphology of the colonies, the shape and dimensions of cells, the thickness and direction of setae, the number and shape of chloroplasts and the presence and morphology of resting spores. However, other features that can

only be resolved with electron microscopy, such as the fine structure of valves and setae and the location and number of rimoportulae, are now considered important (Sunesen et al. 2008). To minimize possible misidentifications, we used both scanning electron microscopy and light microscopy.

Scanning electron microscopy shows that the cells of *Chaetoceros* CEMB, CHAN and BIM were usually solitary with flat or slightly convex valves (Figures. 2d–l). The setae are straight and narrow in diameter and arise from the poles of the cells. The surfaces of the frustules or cell walls were smooth and rectangular in girdle view. *Chaetoceros* CEMB cells were shallow rectangular, whereas those of *Chaetoceros* CHAN and *Chaetoceros* BIM were square to rectangular. Setae size (18.37 ± 7.41 μm) and transapical axis (4.66 ± 1.25 μm) were significantly higher in *Chaetoceros* CEMB than in *Chaetoceros* CHAN and *Chaetoceros* BIM (Table 1). *Chaetoceros* is a centric diatom with lightly silicified frustules. Each frustule possesses four long, thin spines or setae. The setae link the frustules together to form colonies of several cells. Frustules can usually be seen in girdle view. Distinguishing *Chaetoceros* species is difficult using a light microscope. The form of the chains, the sizes of the apical axis and valve shape are some of the most important morphological characters for recognizing species in this genus (Lee et al. 2014). All *Chaetoceros* isolates were confirmed to be *Chaetoceros* based on observation of their morphological features with a scanning electron microscope (Table 2).

Table 1
Morphological characters for differentiating the *Chaetoceros* isolates in this study

Character	*Chaetoceros* CEMB	*Chaetoceros* CHAN	*Chaetoceros* BIM
Cell shape	Shallow rectangular	Square to rectangular	Square to rectangular
Setae shape	Round	Round	Round
Setae size (μm)	11.56–28.93 (18.37 ± 7.41)*	10.25–13.58 (12.01 ± 1.50)	10.27–11.14 (10.62 ± 0.36)
Transapical axis (μm)	3.24–6.16 (4.66 ± 1.25)*	3.50–4.05 (3.70 ± 0.25)	3.27–3.90 (3.53 ± 0.25)
Apical axis (μm)	4.15–8.26 (6.29 ± 1.50)	4.77–6.18 (5.33 ± 0.58)	4.42–5.49 (4.90 ± 0.49)
* indicates statistically significant differences between isolates ($p < 0.05$)			

Table 2
Comparison of the morphological features of *Chaetoceros* CEMB, CHAN and BIM by scanning electron microscopy.

Characteristic	*Chaetoceros* CEMB	*Chaetoceros* CHAN	*Chaetoceros* BIM
Cell	Thick and stiff cells that are shallow rectangular	Thick and stiff cells that are rectangular	Thick and stiff cells that are rectangular
Valve face	Oval	Rectangular to oval	Rectangular to oval
Cell Length	4–8 μm	4–6 μm	4–6 μm
Apical axis	3–6 μm	3–4 μm	3–4 μm
Setae	4 long and thin intercalary setae with rounded terminal parts	4 long and thin intercalary setae with slender terminal parts	4 long and thin intercalary setae with slender terminal parts
Spines	Invisible spine	Invisible spine	Invisible spine

Cells of *C. debilis* are roughly rectangular in girdle view and connected in spiraling chains. The basal part of the setae is distinct, and setae extend outward from the spiral. Valves are flat or slightly convex (although the spines make it appear concave). Apertures are narrowly oval and sometimes slightly constricted in the middle. Their diameter ranges from 8–40 μm; although they are distributed worldwide, they mainly occur in cold waters (Hasle and Syvertsen 1996). Species similar to *C. debilis* include *C. curvisetus*, which forms spirals wider in diameter; in addition, the apertures are larger and widely oval in *C. curvisetus* (Guiry and Guiry 2012; Tas and Hernández-Becerril 2017). The cells of *C. gracilis* and *C. muelleri* have an apical axis that ranges from 6–8 and 8–9 μm and transapical axis that ranges from 3–6 and 6–7 μm, respectively (Olenina et al. 2006). *C. calcitrans* has a cell diameter that ranges from 2–5 μm (Soliman et al. 2010). *C. debilis* is larger than *C. gracilis* and *C. muelleri*. Light and scanning microscope observations showed that *Chaetoceros* CEMB may be a different species compared with *Chaetoceros* CHAN and *Chaetoceros* BIM. Nevertheless, light microscopy is still faster and more reliable for diatom identification in a mixed sample for trained diatomologists.

C. gracilis and *C. calcitrans* are extensively used as food sources for rearing prawn larvae (Chu 1989; Soliman et al. 2010). *C. gracilis* is the phytoplankton species most commonly used in bivalve mollusk and fish hatcheries (Helm et al. 2004). Their effectiveness stems in part from their small size and n-3 HUFA content (Barclay and Zeller 1996).

Nucleotide sequences and 18S rDNA phylogeny of Chaetoceros

The 18S rDNA sequences of *Chaetoceros* were obtained from gene cloning and unidirectional sequencing. *Chaetoceros* CEMB contained 18S rDNA sequences that were 1794 bp in length, which were similar to those of *C. gracilis* (e-value = 0.0, identity = 98%). *Chaetoceros* CHAN had 18S rDNA sequences that were 1788 bp in length, which were similar to those of *C. debilis* (e-value = 0.0, identity = 99%). *Chaetoceros* BIM contained 18S rDNA sequences that were 1789 bp in length, which were similar to those of *C. debilis* (e-value = 0.0, identity = 99%). The 18S rDNA sequences of the three *Chaetoceros* showed high similarity (Fig. 3).

The BLAST analysis revealed high similarity between the *Chaetoceros* sequences obtained in our study and Genbank sequences (Table 3). We characterized nuclear 18S rDNA sequences of three *Chaetoceros* and compared them with available DNA sequences (12 sequences) obtained from GenBank (www.ncbi.nlm.nih.gov). These included complete and partial 18S rDNA sequences. *Chaetoceros* CHAN and BIM were clustered in the same clade with *C. debilis* and *C. curvisetus*, and *Chaetoceros* CEMB was distinct from the others. This result was consistent with morphological data suggesting that *Chaetoceros* CEMB contained significantly larger setae and apical axes than *Chaetoceros* CHAN and BIM. The lack of complete consistency between molecular and morphological identification may stem from morphological shifts that occur between environmental species and cultured ones. Thus, species identification both before and after culture might be required to ensure the accuracy of identification (Kesici et al. 2013).

Table 3
Sequence similarities between 18S rDNA sequences of *Chaetoceros* obtained in this study and GenBank sequences.

Isolate	Morphological identification	18S rDNA similarities	Accession number
Chaetoceros CEMB	*Chaetoceros* sp.	*Chaetoceros gracilis*, e-value = 0.0, identity = 98%	MW513719.1
Chaetoceros CHAN	*Chaetoceros* sp.	*Chaetoceros debilis*, e-value = 0.0, identity = 99%	MW513720.1
Chaetoceros BIM	*Chaetoceros* sp.	*Chaetoceros debilis*, e-value = 0.0, identity = 99%	MW513721.1

Chaetoceros is a diverse genus of marine diatoms. Although the morphology of many members of the genus has been well described, molecular taxonomic studies of *Chaetoceros* are scarce. 18S and 28S rDNA phylogenies indicate that these sequences might provide suitable markers for resolving the species-level taxonomy of *Chaetoceros* (Oh et al. 2010).

RAPD profiles of Chaetoceros

Amplified fragments 300–2000 bp in size were obtained using RAPD-PCR analysis with UBC10 and OPB01 primers (Fig. 5). A dendrogram based on the RAPD-PCR band was created. The RAPD dendrogram was consistent with the 18S rDNA phylogeny shown in Fig. 4.

DNA barcoding requires molecular loci that are variable enough to discriminate species and a molecular reference database for comparison. The similarity or divergence of the molecular sequence of an unknown organism to a vouchered reference sequence in the database is used for species identification. DNA barcoding of environmental samples involves the extraction of DNA from a pooled sample, PCR amplification of a target locus, cloning of the resulting PCR products, sequencing and analysis. With DNA barcoding techniques, even morphologically similar strains can be identified at the species level. These molecular phylogenetic analyses also enable the rapid, convenient and accurate classification of diatoms and have thus contributed considerably to studies of diatom diversity.

RAPD-PCR has been used for the molecular characterization and identification of 17 samples of *Sargassum* spp. (Ho et al. 1995). A 450-bp fragment generated using OPA13 was detected in 12 of 17 samples of *Sargassum*. This fragment was present in profiles from *Turbinaria* (Sargassaceae). This study showed that RAPD-PCR is useful for discriminating *Sargassum* samples and developing fingerprints for them. PCR-RFLP analysis has been used to resolve the species-level differences of 18 isolates of *Chaetoceros* Ehrenberg (Bacillariophyceae) by targeting the *rbc*L region of chloroplast DNA, which encodes the Rubisco large subunit (Toyoda et al. 2013). RAPD patterns for the species-level differences of *Chaetoceros* have not been reported to date.

Molecular identification appears to be relatively effective for diatom identification given the similar efficacies of molecular and morphological identification in this study. However, more work is needed to optimize morphological and molecular approaches for diatom identification.

In the study of the interpopulational variability of the three *Chaetoceros* culture populations, the selection of the RAPD primers was based on the quantity, intensity and repetition of the amplified fragments. These amplified fragments ranged in size from 50 to 2200 bp. A total of 80 fragments were identified, and 113 of these fragments (42.5%) were polymorphic. The average number of fragments per primer was relatively high. The percentage of polymorphic bands was 33.33%, 60.00% and 30.43% for *Chaetoceros* CHAN, *Chaetoceros* CEMB and *Chaetoceros* BIM, respectively (Table 4).

Table 4
Number of RAPD fragments and polymorphic products obtained in the analysis of three *Chaetoceros* populations.

Primer	**Total number of fragments**	**Number of amplified fragments**			**Number of polymorphic fragments**		
		Chaetoceros **CHAN**	Chaetoceros **CEMB**	Chaetoceros **BIM**	Chaetoceros **CHAN**	Chaetoceros **CEMB**	Chaetoceros **BIM**
UBC10	39	14	14	11	5	6	2
OPB01	41	13	16	12	4	12	5
Total	**80**	**27**	**30**	**23**	**9**	**18**	**7**
Polymorphism					**33.33%**	**60.00%**	**30.43%**

Identification of metabolites extracted from Chaetoceros by NMR spectroscopy

The ^{1}H-NMR spectra of methanol extract from all *Chaetoceros* isolates showed similar characteristic chemical shift peaks. There was a total of 27 metabolites that were clearly identified based on comparison with previous research, a free NMR database (The Human Metabolome Database, HMDB) and a commercial NMR database (Bruker AssureNMR). The ^{1}H-NMR spectra shown in Fig. 6 contain different groups of metabolites, including amino acids, sugars, carboxylic acids, fatty acids, vitamins and carotenoids. The peaks corresponding to the structures of each metabolite are summarized in Table 5.

Table 5
The metabolites from *Chaetoceros* methanol crude extract identified by NMR spectroscopy.

Number	Metabolite	Functional Group	Chemical Shift (ppm)
1	Glutamic acid	-CH_2-CH_2-COOH	2.34 (m)
		-CH_2-CH_2COOH	2.13 (m)
		-CH_2-COOH	2.06 (m)
2	Proline	-$(CH_2)_2$-CH-	4.10 (dd)
		-CH_2-	2.32 (m)
		-CH_2-	2.05 (m)
		-CH_2-	1.98 (m)
3	Alanine	(COOH)-CH(CH_3)-NH_2	1.48 (d)
4	Isoleucine	CH_3-CH(CH)CH_2-	0.99 (d)
		CH_3-CH_2-	0.96 (t)
5	Methionine	-CH_2-CH(NH_2)-	2.14 (m)
6	Choline	$(CH_3)_3$N-CH_2-CH_2-OH	4.05 (ddd)
7	Glycine	NH_2-CH_2-COOH	3.54 (s)
8	Cholesterol	-CH_3	0.69 (s)
		-CH(CH_3)$_2$	0.82 (d)
		-CHCH_3	0.87 (d)
		-CHCH_3	0.92 (s)
9	Palmitic acid	-CH_2-COOH	2.31 (m)
		-CH_2-CH_2-CH_2-	1.66 (m)
		-CH_2-(CH_2)$_{14}$-CH_3	1.29 (m)
10	Oleic acid	-CH_2-CH= CH-CH_2-	5.40 (m)
		-CH_2-COOH	2.30 (t)
		-(CH_2)$_n$ -CH_2CH_3	1.93 (m)
		-(CH_2)$_n$-CH_2COOH	1.33 (m)
		-CH_2-CH_3	0.88 (t)

Number	Metabolite	Functional Group	Chemical Shift (ppm)
11	Linolenic acid	-CH_2-C*H*= C*H*-CH_2-	5.38 (m)
		-C*H*$_2$-COOH	2.32 (t)
		-(C*H*$_2$)$_n$-CH_2COOH	1.34 (m)
		-CH_2-C*H*$_3$	0.90 (t)
12	α-linolenic acid	-C*H*= C*H*-	5.36 (m)
		-C*H*$_2$-	2.79 (m)
		-C*H*$_2$-COOH	2.34 (t)
		-C*H*$_2$-	2.04 (m)
		-C*H*$_2$-	1.31 (m)
		-CH_2-C*H*$_3$	0.97 (t)
13	Arachidic acid	-C*H*$_2$-COOH	2.32 (t)
		-C*H*$_2$-CH_2COOH	1.64 (m)
		-C*H*$_2$-CH_3	1.29 (m)
		-CH_2-C*H*$_3$	0.89 (t)
14	Glucose	-C*H*-	5.20 (d)
		-C*H*-	3.82 (m)
		-C*H*$_2$-	3.54 (d)
15	Sucrose	-C*H*-	5.39 (d)
		-C*H*-	4.19 (d)
		-C*H*$_2$-	3.82 (m)
		-C*H*$_2$-	3.67 (s)
		-C*H*-	3.46 (t)
16	Myo-inositol	-C*H*-	4.06 (t)

Number	Metabolite	Functional Group	Chemical Shift (ppm)
17	Fucoxanthin	Olefinic-*H*	6.81 (t)
		Olefinic-*H*	6.74 (dd)
		Olefinic-*H*	6.45 (dd)
		Olefinic-*H*	6.50 (d)
		Olefinic-*H*	6.41 (m)
		Olefinic-*H*	6.10 (m)
		-C*H*-OH	3.65 (m)
		-CH_2-	1.52 (dd)
		-CH_2-	1.38 (dd)
		-CH_3	0.97 (s)
18	Astaxanthin	-C*H*-	7.01 (d)
		Olefinic-*H*	6.20–6.85 (m)
		-CH_2-	4.36 (dd)
		-CH_2-	3.66 (s)
		-CH_3	2.01 (s)
		-CH_3	1.98 (s)
		-CH_3	1.93 (s)
		-CH_3	1.86 (m)
		-CH_3	1.33 (m)
		-CH_3	1.26 (s)
		-CH_3	
19	Lutein	Olefinic-*H*	6.67–6.57 (m)
		Olefinic-*H*	6.38 (d)
		Olefinic-*H*	6.36(d)
		Olefinic-*H*	5.39 (m)
		-C*H*- (eq)	2.35 (m)
		-CH_3	1.19–1.33 (m)
20	Zeaxanthin	-CH_2-	2.02 (s)
		-CH_3	1.99 (s)
		-CH_3	1.68 (s)
		-CH_3	1.06 (s)

Number	Metabolite	Functional Group	Chemical Shift (ppm)
21	Violaxanthin	-C*H*$_2$-	1.93 (s)
		-C*H*$_3$	1.86 (s)
		-C*H*$_3$	1.60 (s)
		-C*H*$_3$	0.92 (s)
22	Chlorophyll c_1	-N*H*-	9.95 (s)
		-N*H*-	9.86 (s)
		-N*H*-	9.77 (s)
		-N*H*-	8.20 (s)
23	Chlorophyll a.	-N*H*-	9.56 (s)
24	Glutamine	-C*H*$_2$-CONH$_2$	2.43 (m)
		-C*H*$_2$-	2.12 (m)
25	Valine	$(CH_3)_2$-C*H*-	2.29 (m)
		-C*H*$_3$	1.03 (d)
		-C*H*$_3$	0.98 (d)
26	Leucine	-C*H*$_3$	1.68 (m)
		-C*H*$_3$	0.94 (d)
27	Stearic acid	-C*H*$_2$	1.73 (t)
		-C*H*$_2$	1.47 (t)
		-C*H*$_3$	1.01 (s)

The characteristic chemical shifts of eight amino acids and sugars were observed around the region 4.10–1.98 ppm, which correspond to the -C*H*$_2$- protons of amino acids, and 1.48–0.96 ppm, which correspond to the -C*H*- and -C*H*$_3$ protons of amino acids (Azizan et al. 2018; Ma et al. 2019; Iglesias et al. 2019). The peaks around 5.20–3.82 ppm correspond to the -C*H*- protons of glucose and sucrose, and the peaks around 3.82–3.67 ppm correspond to the -C*H*$_2$- protons of glucose and sucrose (Richter and Berger 2013). The representative proton signals of fucoxanthin (olefinic-*H*), astaxanthin, lutein and zeaxanthin were observed at a chemical shift around 7.01–6.10 ppm (Zailanie and Purnomo 2017; Shumilina et al. 2020; Otaka et al. 2016; Iwai et al. 2008). The identifications of these carotenoids have been confirmed by 2D-NMR (HMBC and JRES); the JRES spectrum showed the singlet signals of fucoxanthin and astaxanthin at 2.01 and 1.98 ppm, respectively, which correspond to the methyl groups (Fig. 7) (Subramanian et al. 2015). The correlation between the proton and carbon signals in the HMBC spectrum is consistent with the results of previous studies (Azizan et al. 2018) (Figs. 8–9). The signals of chlorophyll a and chlorophyll c_1 observed around 9.77–8.20 ppm correspond to the -N*H*- protons of chlorophyll structures.

^{1}H-NMR and 2D-NMR spectra of the crude extract revealed signals for six fatty acids, including palmitic acid, oleic acid, linoleic acid, α-linolenic acid, arachidic acid and stearic acid (Figs. 10). The characteristic peaks were similar to the results of previous studies (Roswanda et al. 2017; Otto et al. 2014; Singer et al. 1996). The correlation between proton and carbon signals observed around 1.73–1.29 ppm corresponded to arachidic acid, palmitic acid and stearic acid. Other valuable metabolites, such as myo-

inositol, cholesterol and choline, were detected by 1D and 2D NMR spectroscopy. The results indicated that further purification was not required for the identification of some major and minor small metabolites by NMR spectroscopy. Gas chromatography coupled with mass spectrometry (GC – MS) is most widely employed for its separation power, choice of detectors, and the relatively inexpensive cost of the instrumentation. Multiple extraction methods have been developed based on GC – MS techniques according to it allowed the choices of reagent and extraction processes (Zheng et al. 2013). Consequently, NMR spectroscopy is commonly used in metabolomic studies due to its high reproducibility and simple preparation process (Savorani et al. 2013).

Lipids play an important role in larval growth and survival. Eicosapentaenoic acid (EPA) and docosahexaenoic acid (DHA) are considered essential fatty acids because they are integral components of the plasma membrane and marine fish larvae cannot synthesize them from linoleic acid 18:3 (n-3). *M. rosenbergii* also lacks the ability to synthesize linolenic acid and linoleic acid (D'Abramo and Sheen 1993) and has a limited ability to elongate and desaturate short-chain n-3 and n-6 polyunsaturated fatty acids (e.g., C18) to long-chain polyunsaturated fatty acids (e.g., C20) (Reigh and Stickney 1989). *Schizochytrium* spp. contains lipids in amounts as high as 55% of cell weight, of which DHA 22:6 (n-3), EPA 20:5 (n-3) and arachidonic acid represent 35%, 7% and 5%, respectively (Nakahara et al. 1996; Barclay 1997; FAO 2012).

Thus, marine fish larvae must acquire HUFAs through their diet of zooplankton (e.g., rotifers and crustaceans), which are enriched in these nutrients. Increasing the HUFA content of zooplankton before feeding larval fish and shrimp is a regular practice in the aquaculture industry (Apt and Behrens 1999).

Conclusions

This study demonstrates the potential for DNA barcoding, coupled with microscopic observation and NMR characterization, for assessing *Chaetoceros* biodiversity. The RAPD barcodes, 18S rDNA sequences and NMR profiles of the three diatom isolates from this study can be used to identify *Chaetoceros* species when morphological differences are ambiguous.

Declarations

Acknowledgments

We thank the Center of Excellence for Marine Biotechnology (CEMB), Faculty of Science, Chulalongkorn University; Institute of Marine Science, Burapha University (BIM); and Chanthaburi Coastal Fisheries Research and Development (CHAN), Department of Fisheries, Ministry of Agriculture for providing *Chaetoceros*. We thank Mrs. Jantanee Boonmameepool and the Microscopic Center, Faculty of Science, Burapha University for help with scanning electron microscopy.

Funding

This research was financially supported by The Higher Education Commission of Thailand (code 1/2556 Burapha University) to RH.

Conflicts of interest/Competing interests

The authors declare that they have no conflict of interest.

Availability of data and material

Chaetoceros CEMB, NCBI Accession Number = MW513719.1

Chaetoceros CHAN, NCBI Accession Number = MW513720.1

Chaetoceros BIM, NCBI Accession Number = MW513721.1

Code availability

Not applicable

Ethics approval

This research does not contain any studies with animals performed by any of the authors. This research was approved for biosafety by the Institutional Biosafety Committee of Burapha University Thailand.

Consent to participate

Not applicable

Consent for publication

Not applicable

References

1. Altschul, S. F., Gish, W., Miller, W., Myers, E. W. and Lipman, D. J. (1990). Basic local alignment search tool. *Journal of Molecular Biology*. 215: 403-410.
2. Apt, K. E. and Behrens, P. W. (1999). Commercial developments in microalgal biotechnology. *J. Phycol.* 35: 215-226.
3. Azizan, A., Bustamam, M. S.A., Maulidiani, M., Shaari, K., Ismail, I.S. Nagao, N., and Abas, F. (2018). Metabolite Profiling of the Microalgal Diatom Chaetoceros Calcitrans and Correlation with Antioxidant and Nitric Oxide Inhibitory Activities via ^{1}H NMR-Based Metabolomics. *Marine Drugs.* 16: 154.
4. Barclay, W. R. and Zeller, S. (1996). Nutritional enhancement of n-3 and n-6 fatty acids in rotifers and *Artemia nauplii* by feeding spray-dried *Schizichytrium* sp. *Journal of the World Aquaculture Society*. 27: 314-322.
5. Benoiston, A. S., Ibarbalz, F. M., Bittner, L., Guidi, L., Jahn, O., Dutkiewicz, S. and Bowler, C. (2017). The evolution of diatoms and their biogeochemical functions. *Phil. Trans. R. Soc. B*. 372: 20160397.
6. Chu, W. P., McCormick, M. P., Lenoble, J., Brogniez, C. and Pruvost, P. (1989). SAGE II inversion algorithm. Journal of Geophysical Research: Atmospheres. 94: 8339-8351.
7. Evans, K. M., Wortley, A. H. and Mann, D. G. (2007). An Assessment of Potential Diatom “Barcode” Genes (cox1, rbcL, 18S and ITS rDNA) and their Effectiveness in Determining Relationships in *Sellaphora* (Bacillariophyta). *Protist*. 158: 349-364.
8. Fujisawa, T., Fujinaga, S. and Atomia, H. (2017). An *In Vitro* Enzyme System for the Production of myo-Inositol from Starch. *Applied and Environmental Microbiology,* 83(16).
9. Godhe, A., McQuoid, M. R., Karunasagarb, I., Karunasagarb, I. and Rehnstam-Holm, N. S. (2006). Comparison of three common molecular tools for distinguishing among geographically separated clones of the diatom *Skeletonema marinoi* Sarno et Zingone (Bacillariophyceae). *J. Phycol*. 42: 280-291.
10. Guillard, R. R. L. (1975). Culture of phytoplank- ton for feeding marine invertebrates. 26-60.
11. Guiry, M. D. and Guiry, G. M. 2012. *Chaetoceros debilis* Cleve. http://www.algaebase.org /search/species/detail/?species_id=37416. Accessed 18 Mar 2012.
12. Hasle, G. R. and Syvertsen, E. E. (1996). Marine diatoms. (In: Tomas, C. R. ed.) Identifying marine diatoms and dinoflagellates. *Academic Press, Inc., San Diego*. 5-385.
13. Helm, M. M., Bourne, N. and Lovatelli, A. (2004). Hatchery Culture of Bivalves: A Practical Manual. FAO Fisheries Technical Paper Number 471. Rome, Italy. 200.
14. Ho, S.C., Lau, J. and Woo, J. (1995). Life Satisfaction and Associated Factors in Older Hong Kong Chinese. *The American Geriatrics Society*. 43: 252 – 255.
15. Iglesias, M.J., Soengas, R., Probert, I., Guilloud, E., Gourvil, P., Mehiri, M., Lópezd, Y., Cepas, V., Gutiérrez-del-Río, I., Redondo-B., S., Villar, C.J., Lombó, F. Soto, S. and Ortiza F.L. (2019). NMR characterization and evaluation of antibacterial and

antiobiofilm activity of organic extracts from stationary phase batch cultures of five marine microalgae (*Dunaliella* sp., *D. salina*, *Chaetoceros calcitrans*, *C. gracilis* and *Tisochrysis lutea*). *Phytochemistry.* 164: 192-205.

16. Iwai, M., Maoka, T., Ikeuchi, M., and Takaichi, S. (2008). 2,2′-b-Hydroxylase (CrtG) is Involved in Carotenogenesis of Both Nostoxanthin and 2-Hydroxymyxol 2′-Fucoside in *Thermosynechococcus elongatus* Strain BP-1. *Plant and Cell Physiology.* 49(11): 1678-1687.
17. Jensen, K. G. and Moestrup, Ø. (1998). The genus Chaetoceros (Bacillariophyceae) in inner Danish waters. *Opera Botanica*. 133: 5-68.
18. Kajonwattanakul, S., Numnual, W., Sirichaiseth, T. and Wannarangsri, T. (2008). Survey of Marine Phytoplankton in Ship's Ballast Tanks at Laem Chabang International Port, Thailand ASEAN. *Journal on Science and Technology for Development*. 35(1-2): 141-145.
19. Kesici, K., Tüney, I., Zeren, D., Güden, M. and Sukata, A. (2013). Morphological and molecular identification of pennate diatoms isolated from Urla,İzmir, coast of the Aegean Sea. *Turkish Journal of Biology*. 37: 530-537.
20. Ki, J. S. (2009). Comparative molecular analysis of freshwater centric diatoms with particular emphasis on the nuclear ribosomal DNA of *Stephanodiscus* (Bacillariophyceae). *Algae*. 24:129-138
21. Knu, C.V. (2004). A comparison of yield and quality of the rotifer (*Brachionus plicatilis*-L-strain) fed different diets under aquaculture conditions, Vietnam. *Asian Fisheries Science*. 17: 357-363.
22. Ma, N.L., The, K.Y., Ahmad, A., Lam, S.L., Saidon, S.A.B., Husri M.N. and San, C.T. (2019). Metabolite profiling of *Scenedesmus regularis* using nuclear magnetic resonance (NMR). *Malaysian Applied Biology Journal.* 48(1): 117–121.
23. Mendiola, J. A., Torres, C. F., Toré, A., Martin-Álvarez, P. J., Santoyo, S., Arredondo, B. O., Señoráns, F. J., Cifuentes, A. and Ibáñez, E. (2007). Use of supercritical CO_2 to obtain extracts with antimicrobial activity from *Chaetoceros muelleri* microalga. A correlation with their lipidic content. *European Food Research Technology.* 224: 505-510.
24. Oh, H. Y., Cheon1, J. Y., Lee, J. H., Hur, S. B. and Ki, J. S. (2010). Nuclear rDNA characteristics for DNA taxonomy of the centric diatom *Chaetoceros* (Bacillariophyceae). *Algae*. 25(2): 65-70.
25. Olenina, I., Hajdu, S., Edler, L., Andersson, A., Wasmund, N., Busch, S., Göbel, J., Gromisz, S., Huseby, S., Huttunen, M., Jaanus, A., Kokkonen, P., Ledaine, I. and Niemkiewicz, E. (2006). Biovolumes and size-classes of phytoplankton in the Baltic Sea. *BSEP*. 106: 1-144.
26. Otaka, J., Seo, S. and Nishimura, M. (2016). Lutein, a Natural Carotenoid, Induces α-1,3-Glucan Accumulation on the Cell Wall Surface of Fungal Plant Pathogens. *Molecules.* 21: 980.
27. Otto, J.R., Freeman, M.J., Malau-Aduli, B.S., Nichols, P.D., Lane, P.A., and Malau-Aduli, A.E.O. (2014). Reproduction and Fertility Parameters of Dairy Cows Supplemented with Omega 3 Fatty Acid-rich Canola Oil. *Annual Research & Review in Biology*. 4(10): 1611-1636.
28. Otsuka, S., Suda, S., Li, R., Matsumoto, S. and Watanabe, M. (2000). Morphological variability of colonies of Microcystis morphospecies in culture. *J. Gen. Appl. Microbiol*. 46: 39-50.
29. Reigh, R. C. and Stickney, R. R. (1989). Effects of purified dietary fatty acids on the fatty composition of freshwater shrimp *Macrobrachium rosellbergii*. *Aquaculture*. 157- 174.
30. Richter, T. and Berger, S. (2013). A NMR method to determine the anomeric specificity of glucose phosphorylation. *Bioorganic & Medicinal Chemistry.* 21: 2710-2714.
31. Rika Partiwi, A., Dahrul, S., Linawati, H., Lily Maria, G.P. and Maggy, T.S. (2009). Fatty acid synthesis by Indonesian Marine Diatom, *Chaetoceros gracilis*. *HAYATI Journal of Biosciences*. 16(4): 151-156.
32. Rines, J. E. B. and E. C. Theriot (2003). Systematics of Chaetocerotaceae (Bacillariophyceae) I. A phylogenetic analysis of the family. *Phycological Research*. 51: 83-98.
33. Roswanda, R., Putra, I. A., Mujahidin, D. (2017). Dimethyl 9-Octadecenedioate and 9-Oktadecene from Methyl Oleate Via a Ruthenium-Catalyzed Homo Olefin Metathesis Reaction. *International Journal of Technology*. 8(8): 1422.
34. Sambrook, J. and Russell, D.W. (2001). *Molecular Cloning a Laboratory manual*. New York: Cold Spring Harbor.

35. Sangha, M. K., Gupta, P. K., Thapar, V. K, Verma, S. R., Bal, A. S. and Dixit, A. (2000). Agricltural Mechanisation in Asia. *Africa and Latin America (AMA).* 13(1): 54.
36. Savorani, F., Rasmussen, M. A., Mikkelsen, M. S. and Engelsen, S. B. (2013). A primer to nutritional metabolomics by NMR spectroscopy and chemometrics. *Food Res. Int.* 54: 1131–1145.
37. Shumilina, E., Ciampa, A., Ytrestøyl, T. and Dikiy, A. (2020). Assessment of Astaxanthin Accumulation in Hepatocytes of Atlantic Salmon Fed Different Diets Using NMR Spectroscopy. *Molecules*. 25: 1769.
38. Siddall, M. E., Fontanella, F. M., Watson, S. C., Kvist, S. and Ers´eus, C. (2009). Barcoding bamboozled by bacteria: convergence to metazoan mitochondrial primer targets by marine microbes. *Systematic Biology*. 58 (4): 445–451.
39. Singer, S., Sivaraja, M., Souza, K., Millis, K. and Corson, J.M. (1996). ^{1}H-NMR Detectable Fatty Acyl Chain Unsaturation in Excised Leiomyosarcoma Correlate with Grade and Mitotic Activity. *Journal of Clinical Investigation.* 98(2): 244-250.
40. Soliman, F., Glatt, C. E., Bath, K. G., Levita, L., Jones, R. M., Pattwell, S. S. J., Jing, D., Tottenham, N., Amso, D., Somerville, L. H., Voss, H. V., Glover, G., Ballon, D. J., Liston, C., Teslovich, T., Kempen, T. V., Lee, F. S. and Casey, B. J. (2010). A genetic variant BDNF polymorphism alters extinction learning in both mouse and human. *Science.* 327: 863-866.
41. Spaulding, S. and Edlund, M. (2008). Chaetoceros. In Diatoms of the United States. *Retrieved October*. 19: 2017.
42. Subramanian, B., Thibault, M.-H., Djaoued, Y., Pelletier, C., Touaibia, M. and Tchoukanova, N. (2015). *Analyst.* 140: 7423-7433.
43. Sunesen, I., Hernández-Becerril, D. U. and Sar, E.A. (2008). Marine diatoms from Buenos Aires coastal waters (Argentina).V. Species of the genus Chaetoceros. *Revista de Biología Marina y Oceanografía*. 43(2): 303-326.
44. Tamura, K., Dudley, J., Nei, M. and Kumar, S. (2007). MEGA4: Molecular Evolutionary Genetics Analysis (MEGA) software version 4.0. *Molecular Biology and Evolution.* 24:1596-1599.
45. Taş, S. and Hernández-Becerril, D.U. (2017). Diversity and distribution of the planktonic diatom genus *Chaetoceros* (Bacillariophyceae) in the Golden Horn Estuary (Sea of Marmara). *Diatom Research*. 32: 309-323.
46. Thompson, J. D., Higgins, D. G. and Gibson, T. J. (1994). CLUSTAL W: improving the sensitivity of progressive multiple sequence alignment through sequence weighting, position specific gap penalties and weight matrix choice. *Nucleic Acids Res*. 22: 4673-4680.
47. Toyoda, K., Nakasaki, K., Williams, D.M. and Tomaru, Y. (2011). PCR-RFLP Analysis for Species-Level Distinction of The Genus Chaetoceros Ehrenberg (Bacillariophyceae). *Natural Science*. 50: 21-29.
48. Wakana, D., Kato, H., Momose, T., Sasaki, N., Ozeki, Y. and Goda, Y. (2014). NMR-based characterization of a novel yellow chlorophyll catabolite, *Ed*-YCC, isolated from *Egeria densa. Tetrahedron Letters.* 55: 2982-2985.
49. Xu, X., Ji, W., Castell, J.D. and O'Dor, R., (1993). The nutritional value of dietary n-3 and n-6 fatty acids for the Chinese prawn (*Penaeus chinensis*). *Aquaculture*. 118 (3e4): 277-285.
50. Zailanie, K. and Purnomo, H. (2017). Identification of fucoxanthin from brown algae (*Sargassum filipendula*) from Padike village, Talango district, Sumenep regency, Madura islands, using nuclear magnetic resonance (NMR). *International Food Research Journal.* 24(1): 372-378.
51. Zheng, X., Qiu, Y., Zhong, W., Baxter, S., Su, M., Li, Q., Xie, G., Ore, B. M., Qiao, S., Spencer, M. D., Zeisel, S. H., Zhou, Z., Zhao, A. and Jia, W. (2013). A targeted metabolomic protocol for short-chain fatty acids and branched-chain amino acids. *Metabolomics* 9: 818–827.
52. Zhou, Q. C., Li, C. C., Liu, C. W., Chi, S. Y. and Yang, Q. H. (2007). Effects of dietary lipid sources on growth and fatty acid composition of juvenile shrimp, *Litopenaeus vannamei*. *Aquac. Nutr*. 13: 222-229.

Figures

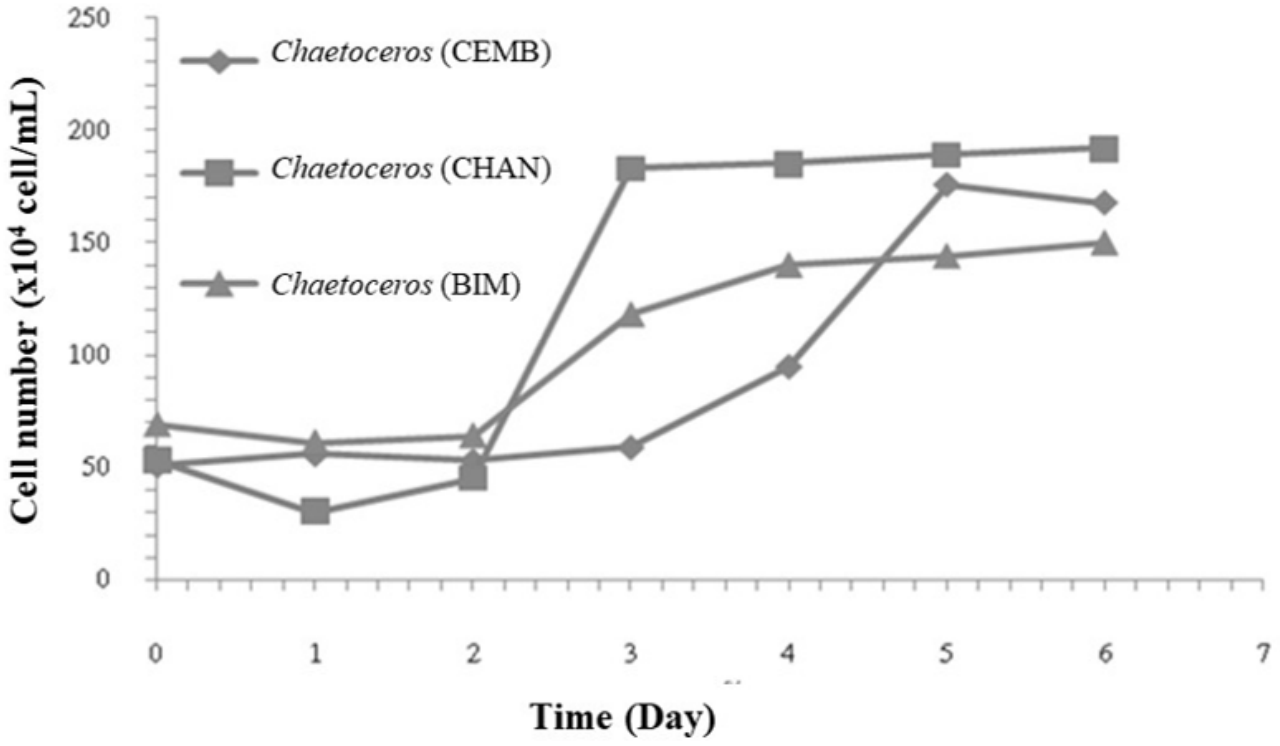

Figure 1

Daily growth curves of three *Chaetoceros* isolates

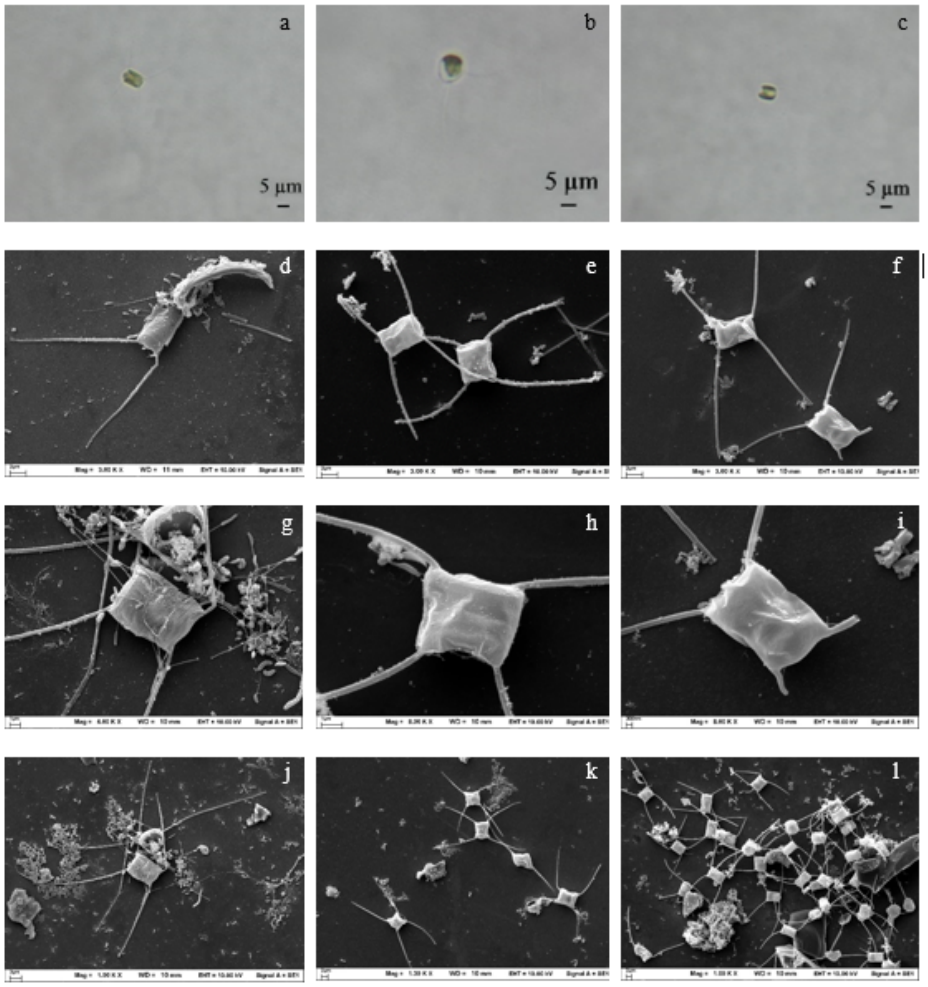

Figure 2

Light (a-c) and scanning electron (d-l) microscope images of *Chaetoceros* CEMB (a, d, g and j), *Chaetoceros* CHAN (b, e, h and k) and *Chaetoceros* BIM (c, f, i and l); the higher magnification shows the shape of entire cells with fibulae and striae (scale bars 5 µm)

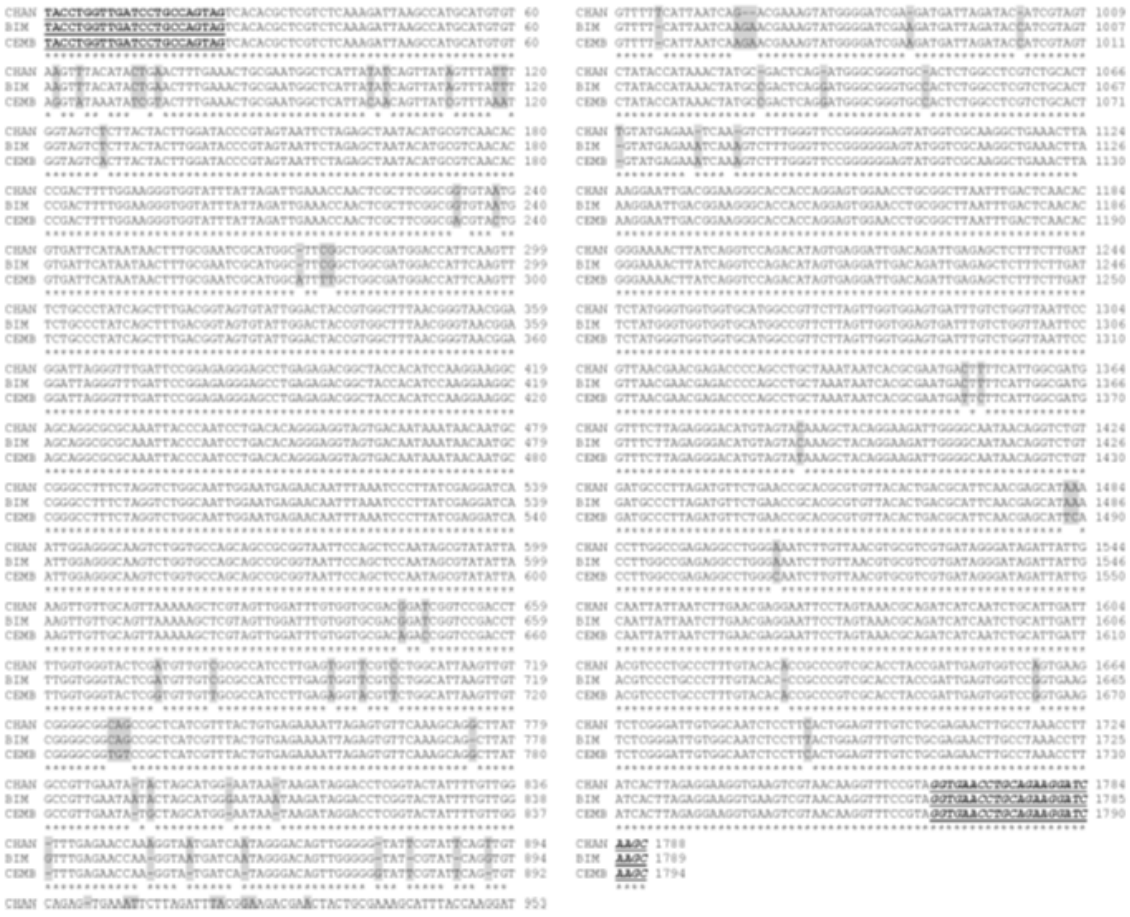

Figure 3

Alignment of 18S rDNA sequences of *Chaetoceros* CHAN, CEMB and BIM using ClustalW2. Highlights show nucleotide differences

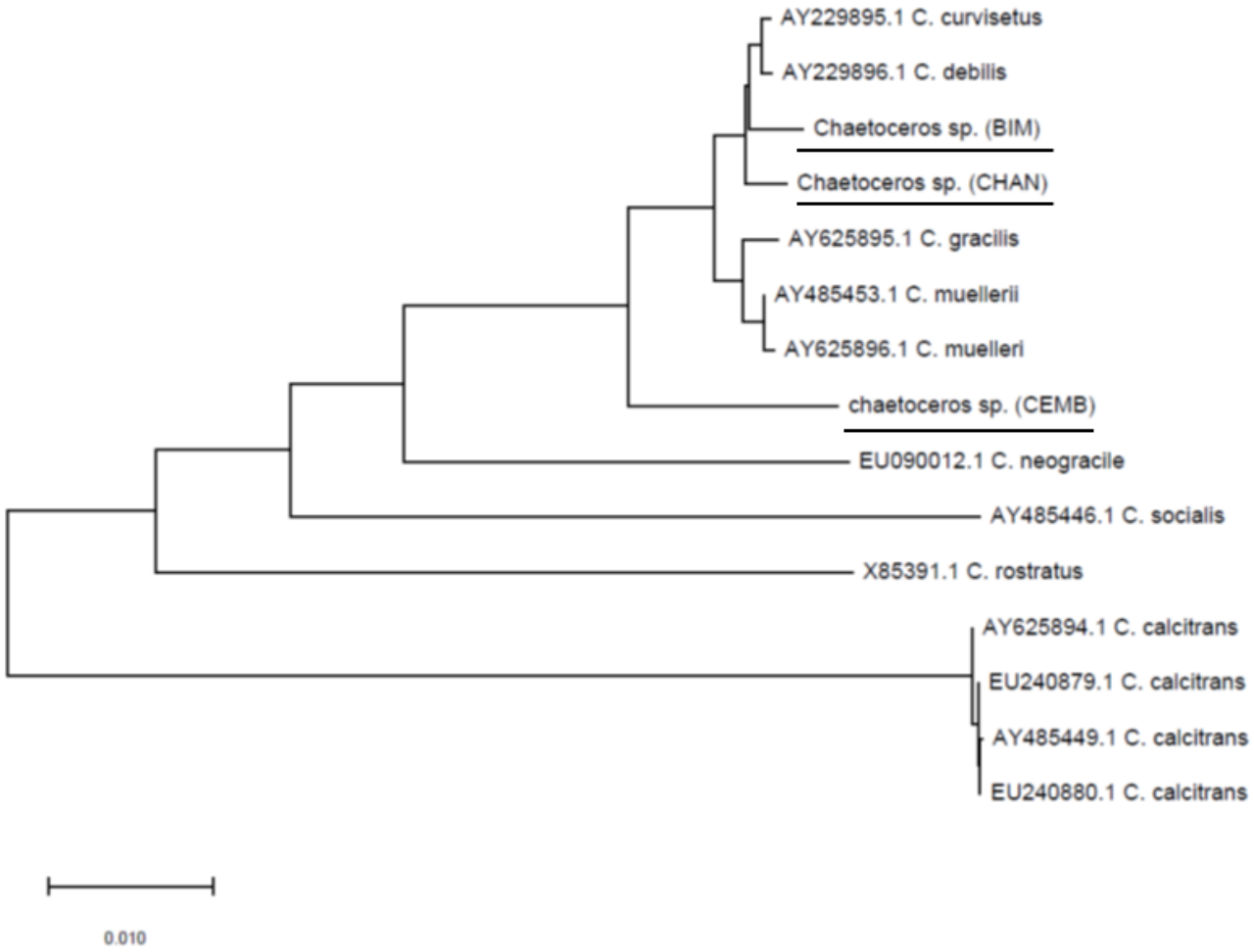

Figure 4

A neighbor-joining phylogeny of *Chaetoceros* CEMB, CHAN and BIM (underlined) and *Chaetoceros* 18S rDNA sequences (12 diatom taxa) from GenBank; 1000 bootstrap replicates were performed to assess the reliability of the topology

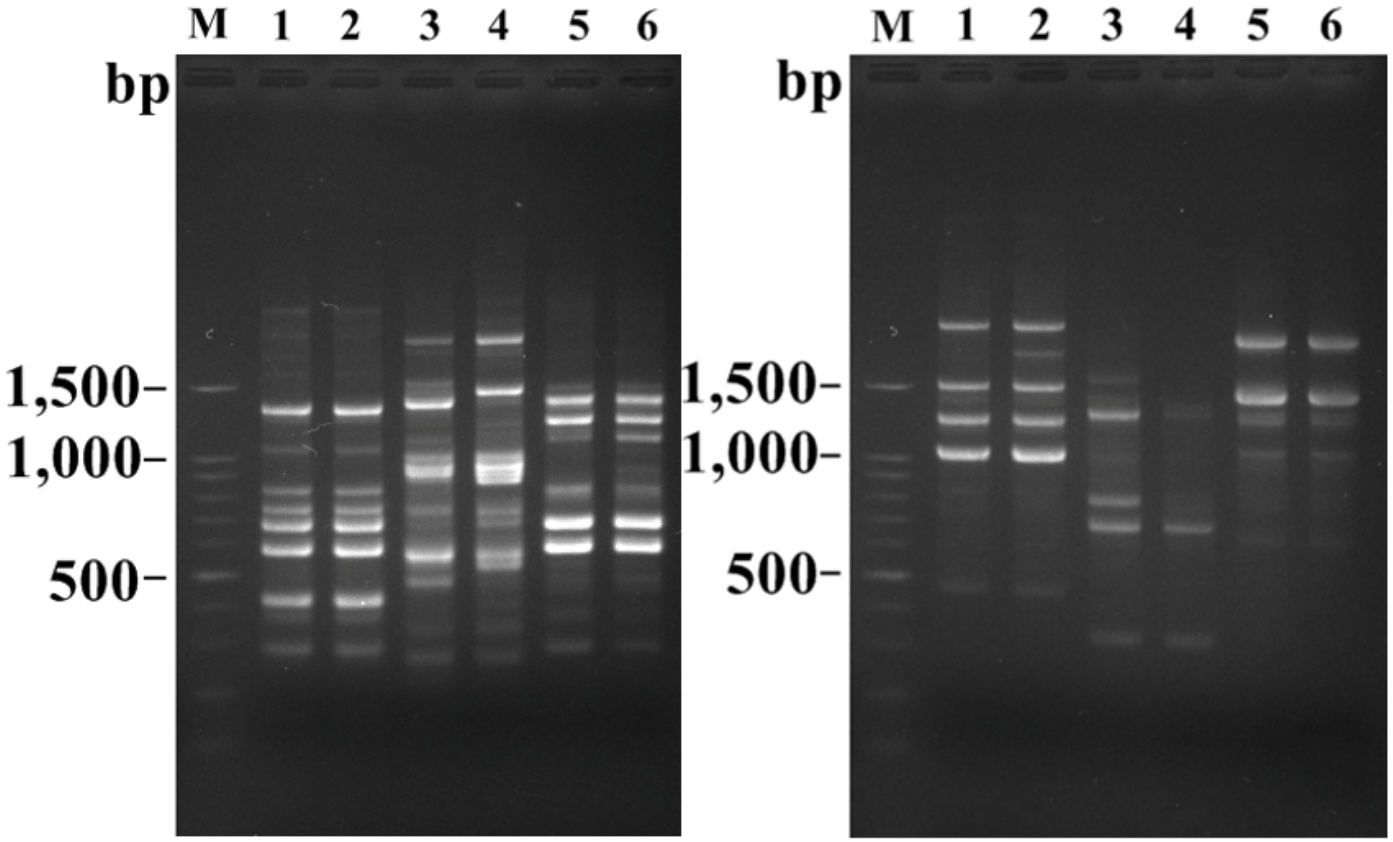

Figure 5

A 2.0% agarose gel showing RAPD patterns of *Chaetoceros* using UBC10 (left) and OPB01 (right). Lanes 1 and 2 *Chaetoceros* CHAN, Lanes 3 and 4 *Chaetoceros* CEMB, Lanes 5 and 6 *Chaetoceros* BIM; M is the 100 bp DNA Marker

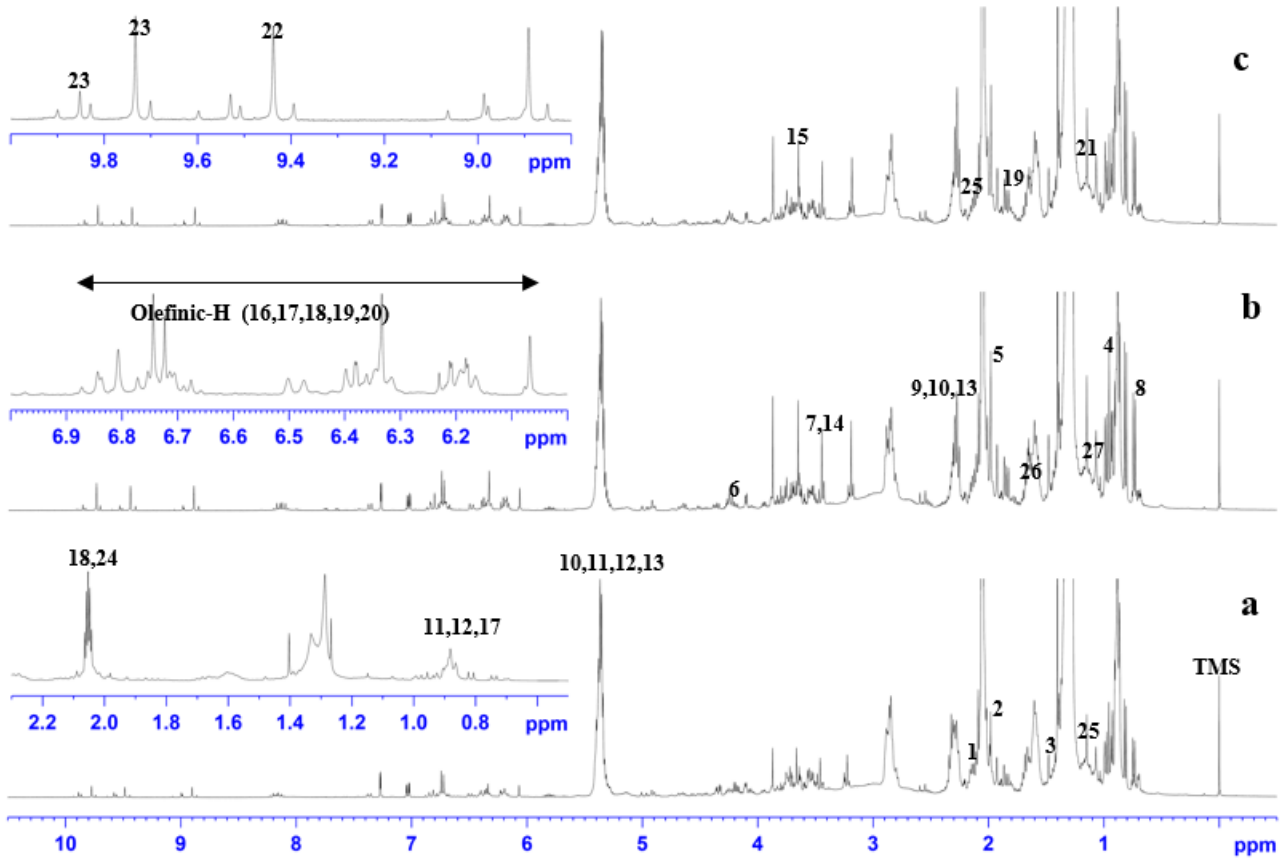

Figure 6

^{1}H-NMR spectra of *Chaetoceros* methanol extract in acetone-D_6 : (a) *Chaetoceros* CEMB (b) *Chaetoceros* BIM and (c) *Chaetoceros* CHAN where 1, glutamate; 2, proline; 3, alanine; 4, isoleucine; 5, methionine; 6, choline; 7, glycine; 8, cholesterol; 9, palmitic acid; 10, oleic acid; 11, linolenic acid; 12, α-linolenic acid; 13, arachidic acid; 14, glucose; 15, sucrose; 16, myo-inositol; 17, fucoxanthin; 18, astaxanthin; 19, lutein; 20, zeaxanthin; 21, violaxanthin; 22, chlorophyll c_1; 23, chlorophyll *a*.; 24, glutamine; 25, valine; 26, leucine; and 27, steric acid

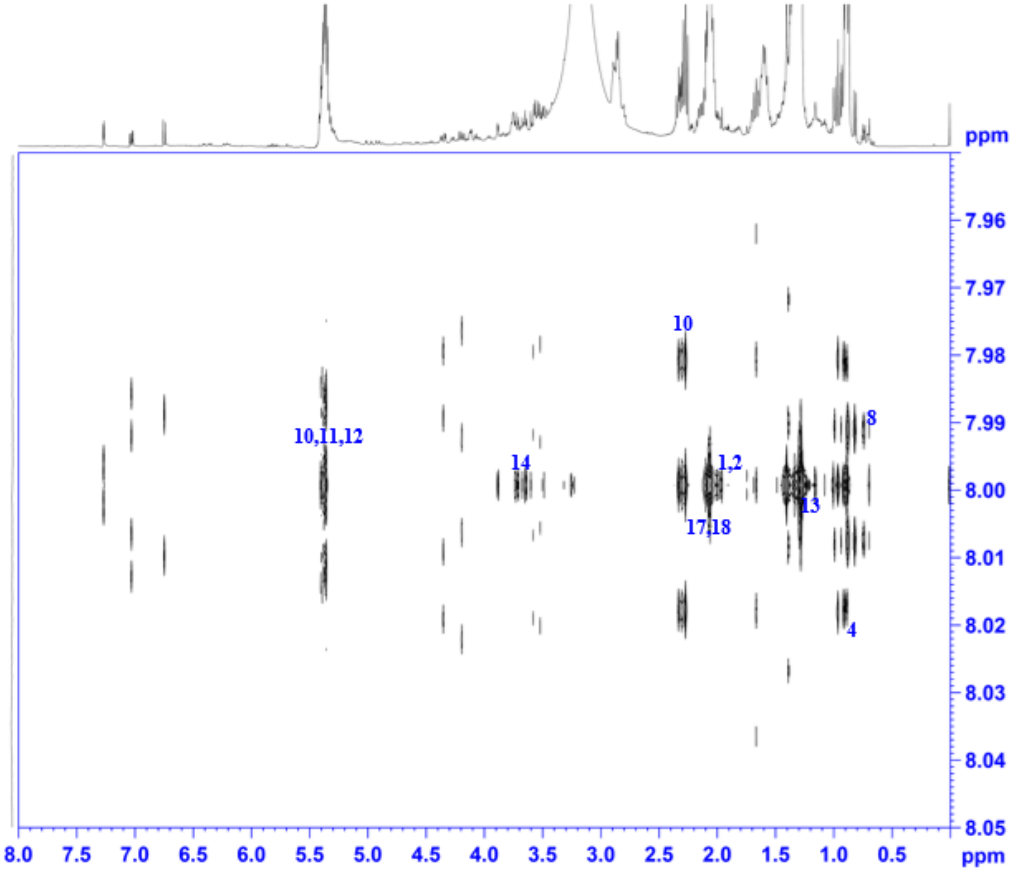

Figure 7

2D J-Resolved NMR spectrum of *Chaetoceros* CEMB in acetone-D_6 where 1, glutamate; 2, proline; 3, alanine; 4, isoleucine; 5, methionine; 6, choline; 7, glycine; 8, cholesterol; 9, palmitic acid; 10, oleic acid; 11, linolenic acid; 12, α-linolenic acid; 13, arachidic acid; 14, glucose; 15, sucrose; 16, myo-inositol; 17, fucoxanthin; 18, astaxanthin; 19, lutein; 20, zeaxanthin; 21, violaxanthin; 22, chlorophyll c_1; 23, chlorophyll *a*.; 24, glutamine; 25, valine; 26, leucine; and 27, steric acid

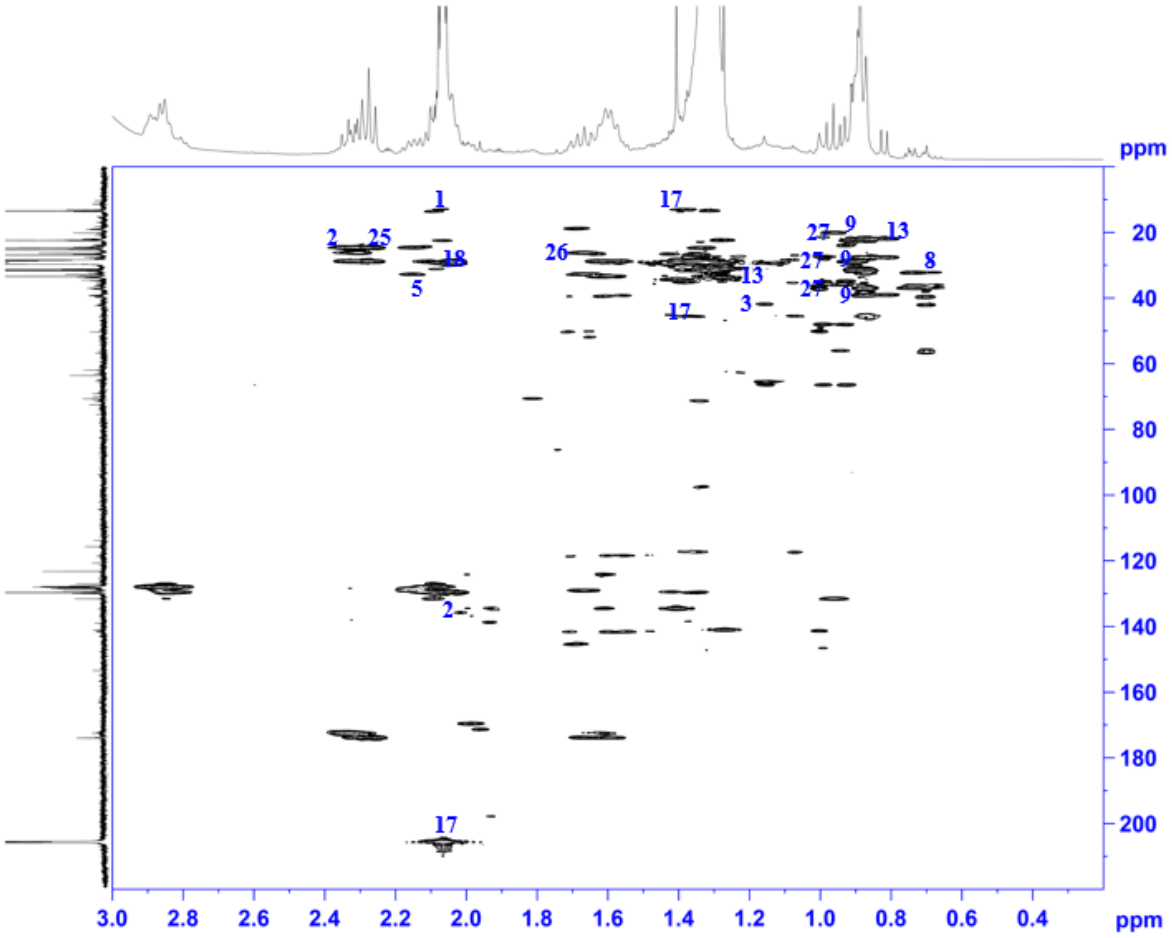

Figure 8

^{1}H-^{13}C HMBC-NMR spectrum of *Chaetoceros* BIM in acetone-D_6 (up-field region) where 1, glutamate; 2, proline; 3, alanine; 4, isoleucine; 5, methionine; 6, choline; 7, glycine; 8, cholesterol; 9, palmitic acid; 10, oleic acid; 11, linolenic acid; 12, α-linolenic acid; 13, arachidic acid; 14, glucose; 15, sucrose; 16, myo-inositol; 17, fucoxanthin; 18, astaxanthin; 19, lutein; 20, zeaxanthin; 21, violaxanthin; 22, chlorophyll c_1; 23, chlorophyll *a*.; 24, glutamine; 25, valine; 26, leucine; and 27, steric acid

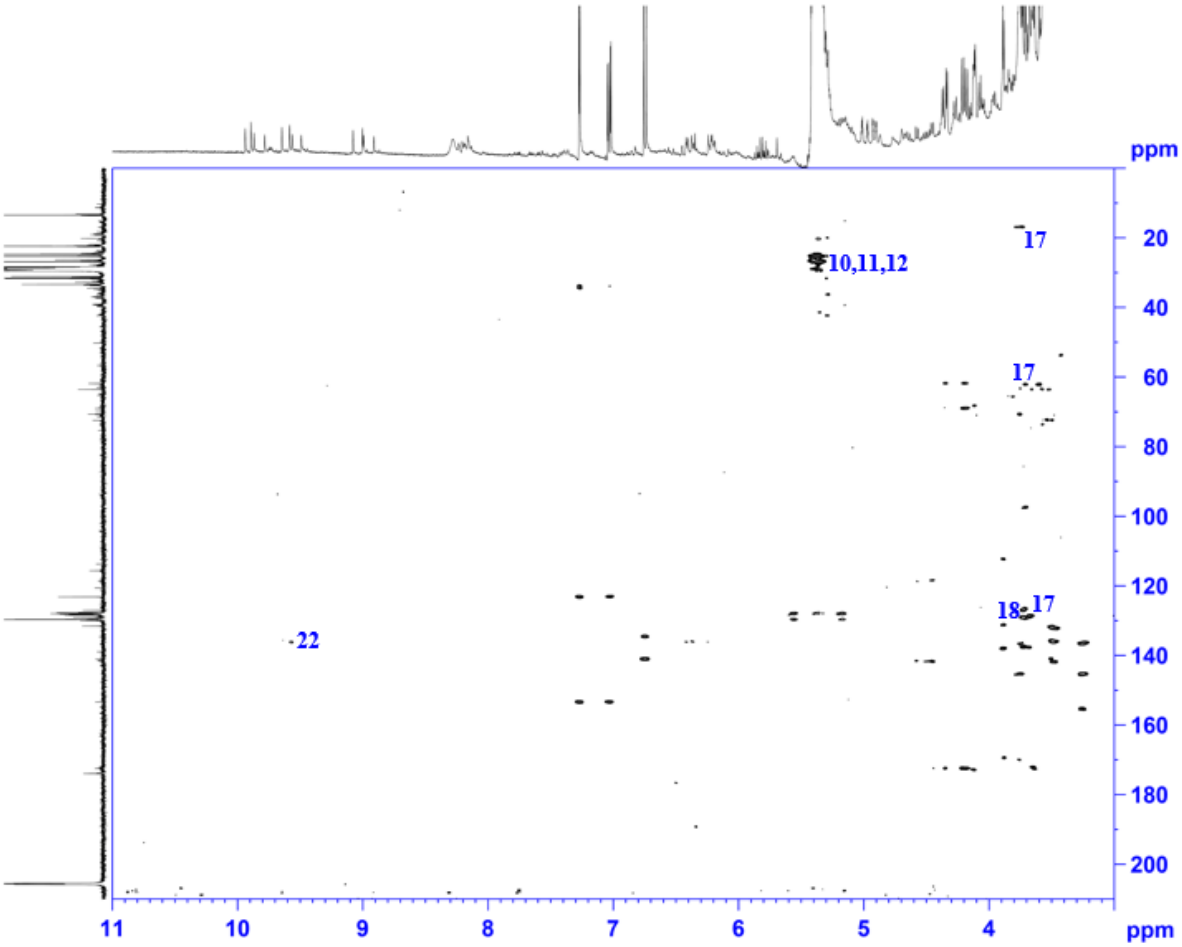

Figure 9

^{1}H-^{13}C HMBC-NMR spectrum of *Chaetoceros* CHAN in acetone-D_6 (down-field region) where 1, glutamate; 2, proline; 3, alanine; 4, isoleucine; 5, methionine; 6, choline; 7, glycine; 8, cholesterol; 9, palmitic acid; 10, oleic acid; 11, linolenic acid; 12, α-linolenic acid; 13, arachidic acid; 14, glucose; 15, sucrose; 16, myo-inositol; 17, fucoxanthin; 18, astaxanthin; 19, lutein; 20, zeaxanthin; 21, violaxanthin; 22, chlorophyll c_1; 23, chlorophyll *a*.; 24, glutamine; 25, valine; 26, leucine; and 27, steric acid

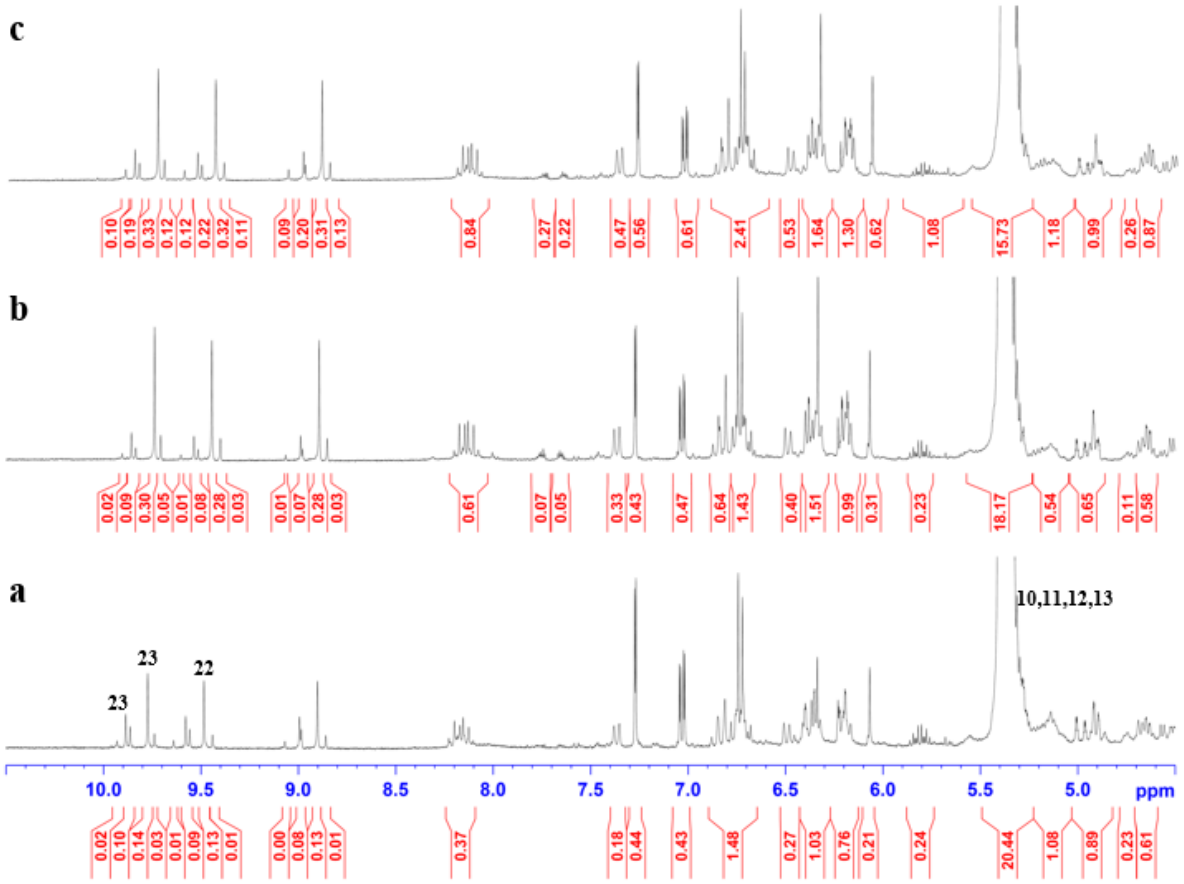

Figure 10

Expanded ^{1}H-NMR spectra of *Chaetoceros* methanol extract with the peak area (ratio) compared with the 0.03% TMS peak area in acetone-D_6: (a) *Chaetoceros* CEMB (b) *Chaetoceros* BIM and (c) *Chaetoceros* CHAN where 10, oleic acid; 11, linolenic acid; 12, α-linolenic acid; 13, arachidic acid; 22, chlorophyll c_1; 23, chlorophyll *a*.; 24, glutamine; 25, valine; 26, leucine; and 27, steric acid